

Implant-to-Wearable Communication through the Human Body: Exploring the Effects of Encapsulated Capacitive and Galvanic Transmitters

Anyu Jiang¹, Cassandra Acebal², Brook Heyd¹, Trustin White¹, Gurleen Kainth², Arunashish Datta³, Shreyas Sen³, Adam Khalifa¹ and Baibhab Chatterjee¹

¹Dept. of ECE., University of Florida, Gainesville, USA. ²Dept. of BME, University of Florida, Gainesville, USA

³School of ECE, Purdue University, West Lafayette, USA

email: {anyu.jiang, chatterjee.b}@ufl.edu

arXiv:2406.13141v1 [q-bio.TO] 19 Jun 2024

Abstract—Data transfer using human-body communication (HBC) represents an actively explored alternative solution to address the challenges related to energy-efficiency, tissue absorption, and security of conventional wireless. Although the use of HBC for wearable-to-wearable communication has been well-explored, different configurations for the transmitter (Tx) and receiver (Rx) for implant-to-wearable HBC needs further studies. This paper substantiates the hypothesis that a fully implanted galvanic Tx is more efficient than a capacitive Tx for interaction with a wearable Rx. Given the practical limitations of implanting an ideal capacitive device, we choose a galvanic device with one electrode encapsulated to model the capacitive scenario. We analyze the lumped circuit model for in-body to out-of-body communication, and perform Circuit-based as well as Finite Element Method (FEM) simulations to explore how the encapsulation thickness affects the received signal levels. We demonstrate in-vivo experimental results on live Sprague Dawley rats to validate the hypothesis, and show that compared to the galvanic Tx, the channel loss will be ≈ 20 dB higher with each additional mm thickness of capacitive encapsulation, eventually going below the noise floor for ideal capacitive Tx.

Index Terms—Capacitive, Galvanic, HBC, BAN, Data Transfer

I. INTRODUCTION

Implanted devices, such as smart glucose monitors and pacemakers, play an important role in managing certain health conditions in an effective manner. These devices can form a closed-loop system with an external smart hub on the human body, enabling the detection of specific health indicators. This integration leads to personalized therapies with continuous monitoring, offering significant advancements in patient care.

Currently, the wireless communication between implantable Tx and external Rx mostly relies on radio frequency (RF) protocols such as Bluetooth or Wi-Fi. Because such traditional wireless techniques utilize high-frequency signals through a lossy medium (air), the energy-efficiency is usually poor (≈ 1 nJ/bit [1]), leading to frequent replacement of any battery in the Tx, or the need for better harvesting techniques. Additionally, traditional wireless gets absorbed in the body, and has a significant amount of electromagnetic (EM) leakage outside the body, making it susceptible to hacking [2]. HBC has emerged as a potential solution to these challenges, utilizing the body's conductive properties for secure, low-power data transmission [3], [4]. At Electro-quasistatic (EQS) frequencies

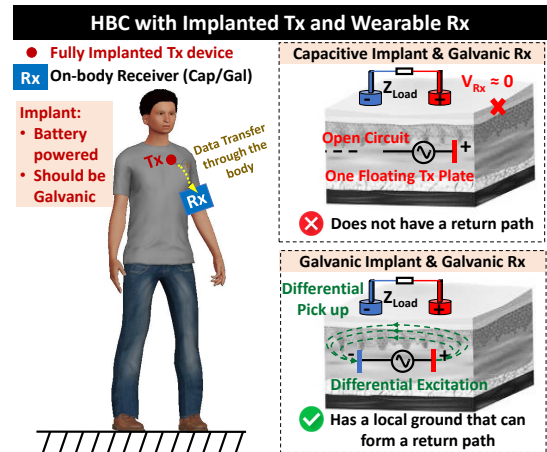


Fig. 1. HBC for implanted Tx (capacitive/galvanic). Ideal capacitive Tx has no signal return path, which would result in almost no signal at the Rx. Note that only a galvanic Rx is shown (Rx can be either capacitive or galvanic).

(< 10's of MHz), HBC offers low-power and secure communication between devices in, on or around the body.

HBC technology, based on its signal coupling mechanisms, can be classified into two primary categories: capacitive [3] and galvanic [4]. Capacitive HBC operates through single-electrode coupling at the Tx and Rx, and transfers electrical signals through the forward path within the human body. The return path is formed by the parasitic capacitances between the earth ground and the local reference/ground planes in the Tx and Rx, as well as the parasitic capacitance formed between the human body and the earth ground [5]. For galvanic HBC, on the other hand, the Tx and Rx are differential (coupled to the body using two electrodes/dipole coupling). The electric fields generated in the Tx flow through the body and are subsequently captured by the differential receiving device.

For wearable applications, capacitive HBC is a safe and simple approach. However, importantly, for a fully implanted HBC device, a capacitive Tx will incur a significantly higher amount of loss as the local ground plane at the Tx will not have a direct parasitic return path to the earth ground [6], [7].

As shown in Fig.1, a capacitive fully implanted Tx does not form a close loop signal path with the Rx, leading to the Rx voltage ≈ 0 . Consequently, a fully implanted Tx needs to be galvanic. In practical scenarios, implanting an ideal

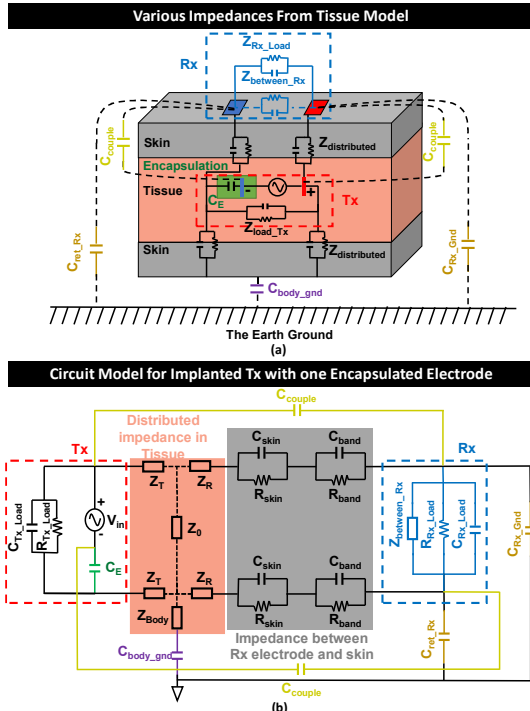


Fig. 2. (a) Tissue and skin impedance model with implanted Tx (with one encapsulated electrode) and galvanic Rx. (b) Circuit model of (a). Note that the impedances inside the body are distributed in reality.

capacitive Tx with a floating reference electrode that doesn't interact with the surrounding tissue is hard to achieve. One approach to model the capacitive scenario is to encapsulate the reference electrode of a galvanic Tx. Depending on the encapsulation material and thickness, the reference electrode on the Tx can still excite the tissue through capacitive dipole coupling. However, if the encapsulation is thick enough, the Tx can be considered as capacitive.

An extremely important consideration for measuring in-vivo HBC performance for implants is that the setup should have a fully implanted Tx with closed surgical wounds, which would ensure that no component of the Tx (not even the battery or any wires) is outside the body, which would otherwise capacitively couple with the Rx, and offer optimistic results even in the capacitive Tx scenarios through additional coupling [8], [9]. Additionally, encapsulating the reference electrode in the Tx may not ensure capacitive HBC operation, as galvanic dipole coupling will still be dominant with some additional loss due to the encapsulation, very similar to the biphasic coupling scenarios [7], [10].

In this paper, we explore the channel transfer function (TF) for both a galvanic and capacitive (galvanic with the reference electrode encapsulated) Tx, along with supporting results from an equivalent circuit model, FEM simulations as well as in-vivo experiments. The contributions of this study are highlighted as follows:

- Developed a **circuit model** for fully implanted Tx and wearable Rx, based on the impedances present for in-body to out-of-body signal transfer, which explains how the encapsulation thickness for the reference electrode on the Tx affects the channel loss. Circuit simulations in

Cadence show why an ideal capacitive Tx is unsuitable.

- Performed **FEM simulations** for the implant in a simplified rat EM model with multiple tissue layers using Ansys High Frequency Structure Simulator (HFSS).
- Finally, developed a fully implanted, flexible signal generator as an HBC Tx and performed **in-vivo experiments** with galvanic as well as encapsulated Tx in live Sprague Dawley rat models to observe channel losses. This crucial measurement confirms that the theory holds true in a living organism. The fully implanted Tx helps in avoiding any parasitic capacitive effects during signal transfer.

The rest of the paper is organized as following: Section II presents a critical analysis of the circuit model and FEM simulation results for capacitive (encapsulated) vs galvanic HBC. Section III details the setup and results of the in-vivo measurements. Finally, Section IV concludes the paper.

II. THEORY, ANALYSIS AND SIMULATIONS

An implanted capacitive Tx (with one encapsulated and one unencapsulated electrode) will suffer from a significantly high loss at EQS frequencies (10s' of MHz or lower). In this section, the circuit model for such scenarios is analyzed based on implanted encapsulated Tx and wearable galvanic Rx. The modality of the wearable Rx will not have a strong impact on the working principle of the Tx [6]. The effect of encapsulation can be observed through circuit-level simulation of an electrical model in Cadence as well as through FEM simulation of a rat model in HFSS.

A. Implanted Tx Circuit Model

There have been recent studies [5], [11] to characterize the circuit model of both capacitive and galvanic Tx/Rx in wearable scenarios. Such circuit models utilize impedances based on the design of the Tx and Rx, as well as tissue impedances and parasitic impedances (return paths to earth ground for capacitive HBC), the values for which are calculated based on the permittivity and conductivity of the tissue and surrounding media [12], along with real measurements. For an implanted Tx, the circuit models needed to be updated. Also, previous models are based on the tissue dielectric properties at 100's of kHz, which means that the value for each component needs to be scaled when it is operated at any other frequency, such as $\sim 21\text{MHz}$ (IEEE 802.15.6 standard for body area networks).

The different impedances in the circuit model is shown in Fig.2(a). The Tx directly couples signal to the tissue using two electrodes in the galvanic scenario, while the encapsulation in capacitive scenario is modeled by the capacitance, C_E on the reference electrode of the Tx. The Tx is loaded by parallel tissue impedances, which are modeled by the parallel RC to the Tx. As shown in Fig.2(b), a distributed tissue impedance model is considered from the Tx electrodes to the skin layer under the Rx electrode. In reality, the impedance value will vary with the distance from Tx to Rx. Because the capacitance in between is low, the tissue of the forward path can be simplified as resistance dominated. The skin layer and the interface of the Rx electrodes with the skin are represented as

parallel RC. Additionally, the inherent parallel RC load at the Rx device, along with a parallel resistance between the 2 Rx electrodes (representing the conductive path through the skin) will form the total Rx load, note that the resistance between can be adjusted by changing the distance.

In addition to the differentially coupled signal path between the Tx and Rx, there will be parasitic capacitance from the wearable Rx electrodes to the earth's ground (C_{ret_Rx} and C_{Rx_Gnd} , as shown in [5]), as well as parasitic capacitances representing inter-device coupling C_{Couple} between the Tx and Rx. These parasitic capacitances introduce additional coupling from Tx to Rx. However, unlike the capacitive wearable HBC case, they are not necessary for forming any closed-loop path for signal transfer, when both the Tx and the Rx are galvanic.

To model the encapsulation on the reference electrode of the Tx, a series capacitor (C_E) is introduced at the local ground of the Tx. In theory, the thicker the encapsulation, the smaller will be the value of C_E (larger impedance), leading to additional loss. Considering the electrode and the encapsulation as two concentric cylinders, the capacitance of this configuration can be computed, typically within the pF range.

In the limiting scenario, $C_E = 0$ (infinite encapsulation) behaves like an open circuit. As a result of such single-electrode coupling, the Tx can be considered as capacitive, leading to very weak Rx signals, as the entire voltage drop happens across the impedance due to C_E .

B. Simulation Setup and Result

To validate the effect of encapsulating one electrode in the Tx, a circuit-EM co-simulation for channel loss was performed. This involved a lumped circuit model simulation using Cadence, coupled with FEM simulations in Ansys HFSS.

1) *Simulation Setup:* The lumped element circuit model of encapsulated Tx and galvanic Rx is shown in Fig.2(b). To analyze loss at frequencies ≈ 21 MHz, component values are estimated based on the Gabriel model [12] and [5]. To align the encapsulation thickness effect to the Rx signal, the value of C_E was adjusted within pF range. The channel loss was measured near 21 MHz according to the IEEE 802.15.6 standard.

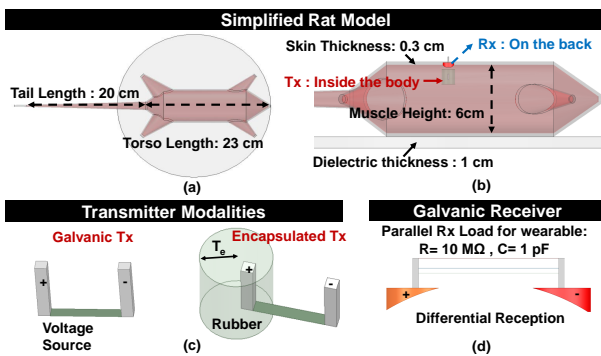


Fig. 3. (a) Top view and (b) side view of the simplified rat model, showing the implementation of Tx and Rx. (c) Pure galvanic Tx and encapsulated Tx to mimic the capacitive implant Tx. (d) The Galvanic Rx model.

Also, a simplified model of a rat made of skin and muscle tissue is created in HFSS for the EM simulation, which is shown in Fig.3(a)-(b). First, a galvanic Tx is placed inside

the rat's body while a galvanic Rx is placed on the skin of the rat. The Tx excites the tissue differentially with a 1 V lumped voltage source applied. The Rx voltage is calculated by integrating the electric field along an integration line between the Rx electrodes. Next, a hard rubber ($\epsilon = 3$) is attached around the Tx reference electrode to make the Tx act capacitively. The encapsulation thickness will be adjusted to observe its corresponding effect on channel loss, which is the ratio of Rx voltage to Tx voltage for voltage-mode HBC.

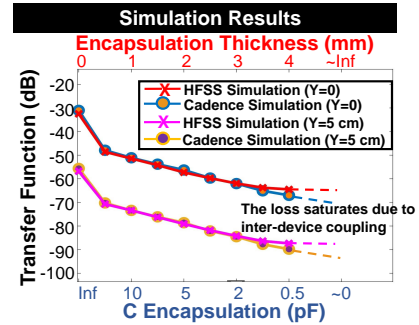


Fig. 4. Simulation Result for the encapsulated Tx with both HFSS and Cadence. The x-axis is the encapsulation thickness (or the value of C_E).

2) *Simulation Result:* The simulation results, as illustrated in Fig.4, explain the correlation between the channel loss and either the value of C_E or the thickness of encapsulation. Key observations include the following: Initially when the encapsulation is thin (C_E is large), a substantial amount of signal can still be received through dipole coupling. As the encapsulation gets thicker, C_E decreases, introducing greater impedance as well as signal loss at the encapsulation, causing the Rx voltage to drop. In the extreme scenario of very thick encapsulation, the coupling between the encapsulated electrode and the tissue becomes negligible, indicating that $C_E \approx 0$. Hence, the Tx can be considered as capacitive, leading to its inefficacy for implantation purposes. Additionally, depending on the distance between the Rx and Tx, still a considerable amount of signal can be detected due to inter-device coupling, which sets a saturation limit in the channel loss even when $C_E \approx 0$, or equivalently, when the encapsulation becomes significantly thick, as seen from the simulations.

III. IN-VIVO EXPERIMENT

The in-vivo experiments were conducted using anesthetized Sprague Dawley rats over multiple days according to proper Institutional Animal Care and Use Committee (IACUC) guidelines at University of Florida, and repeatable results are reported. The experiments confirm that there is a corresponding increase in channel loss as the encapsulation on one electrode of the galvanic Tx gets thicker. This hypothesis holds true for both capacitive and galvanic Rx on the rat's body.

1) *Experiment Setup:* The in-vivo experimental set up is detailed in Fig.5. The Rx consists of a handheld spectrum analyzer (SA) connecting to a 50Ω buffer (Texas Instruments BUF602). This buffer drives the 50Ω SA while offering high-impedance termination at the body [6]. A 3×4 electrode array, made with flexible Polyimide PCB, is connected to the skin

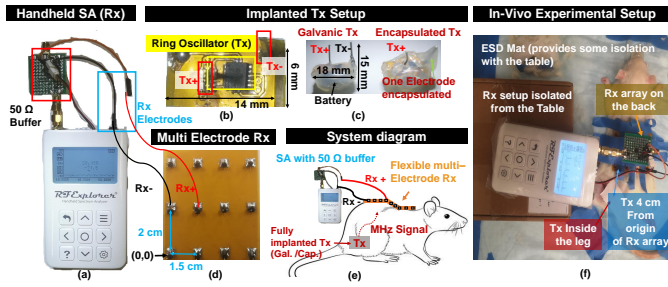


Fig. 5. (a) RF Explorer handheld spectrum analyzer (SA) with $50\ \Omega$ buffer, connecting to a multi-electrode Rx. (b) The Flexible Tx Implant, featuring a battery-powered ring oscillator. (c) Side view of the set up, showing galvanic Tx and encapsulated Tx. (d) Multi electrode array taped on the rat's back to measure Rx signal. (e) Full system diagram. (f) In-vivo measurement setup.

of the rat's back for robust and reconfigurable signal reception at various locations. Each electrode on the array is a square with $5\text{mm} \times 5\text{mm}$ surface area.

The fully implanted galvanic Tx is designed on a flexible Polyimide PCB using the SN74AHC04BQAR inverter. By setting the Tx as a 3-stage ring oscillator, ≈ 21 MHz signal can be generated. The galvanic Tx has 2 exposed electrodes, while the remaining parts are sealed to ensure waterproofing. To mimic the conditions of a capacitive implant, the reference electrode is coated with glue to prevent direct contact with the rat's tissue. To ensure the accuracy of the results, both the rat and the Rx are isolated from the table, minimizing potential earth coupling [10].

For the experiments, both female and male adult Sprague Dawley rats were used. Throughout the surgical process, the rats were anesthetized with 1%–3% isoflurane. The surgical procedure involved an incision that ran from the knee joint to the ischial tuberosity to expose the muscle of the leg of the rat. After that, the Tx will be placed under the skin, with the surgical wound closed, with one (capacitive) or two (galvanic) Tx electrodes making direct contact with the muscle tissue.

The experiment measures the channel loss on the back of the rat with a fully implanted Tx. The bottom left corner pin of the multi-electrode Rx was considered as the origin for the coordinate system, the Rx can alternate between capacitive and galvanic modes by connecting either one or two electrodes. This setup allows for the observation and measurement of channel loss variations in response to changing the encapsulation thickness of the Tx as well as the modality of Rx. At the experimental endpoint, each rodent was euthanized.

2) *Experimental Results:* The experimental results are shown in Fig. 6. The channel loss measured along the back of the rat is shown as a surface plot. For both capacitive and galvanic Rx, as the encapsulation gets thicker, the channel loss keeps increasing at a rate of $\approx 20\text{dB}$ per mm of encapsulation, eventually going below the SA noise level (> 80 dB loss). As the encapsulation thickness increases, the implant begins to behave more like a capacitive Tx, and a high channel loss is observed. This trend is consistent with the data from the simulation shown in Fig.4 (although the slope is different because of slight material property mismatch), thereby validating the measurements obtained in the experiment. Also,

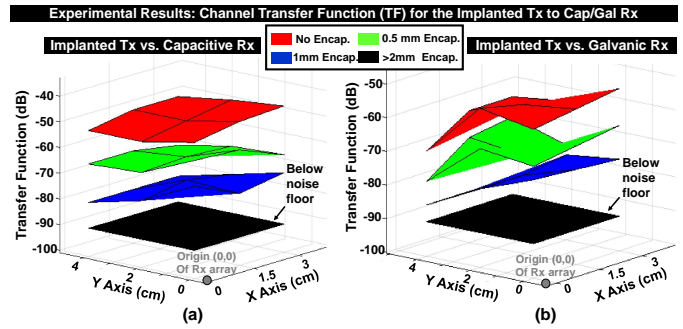


Fig. 6. 3D plot for Tx with different thickness of encapsulation versus (a) Capacitive Rx, (b) Galvanic Rx with electrodes spaced 1.5 cm apart, moving along the back. Note that if the encapsulation is greater than 2 mm, the Rx signal will be below the noise level and the channel loss will be greater than 85 dB.

the trend of the channel loss corresponding to the 2D distance from Tx with different modality of Rx matches with previous study [6] - with increasing distance, capacitive Rx exhibits a saturation in channel loss, whereas galvanic Rx shows a continuous reduction in the channel TF.

IV. CONCLUSION

We have investigated the effects of capacitive and galvanic Tx for implant-to-wearable scenarios in HBC using a proposed lumped circuit model, FEM simulations and in-vivo measurements, which demonstrate well-aligned results. The in-vivo experiment has been performed with both capacitive (encapsulated) and galvanic Tx and Rx. The experimental results indicate that with 1 mm encapsulation on one of the Tx electrodes, ≈ 20 dB loss will be added compared to a pure galvanic Tx. With $> 2\text{mm}$ encapsulation thickness, the Rx signal goes below the noise levels. This study substantiates the hypothesis that, in implant-to-wearable scenarios, a galvanic Tx proves more efficient, while a fully implanted capacitive Tx is not feasible for effective interaction with a wearable Rx.

REFERENCES

- [1] B. Chatterjee, P. Mohseni, and S. Sen, "Bioelectronic Sensor Nodes for the Internet of Bodies," *Annual Review of Biomed. Eng.*, 2023.
- [2] D. Das *et al.*, "Enabling Covert Body Area Network using Electro-Quasistatic Human Body Communication," *Scientific Reports*, 2019.
- [3] T. G. Zimmerman, "Personal Area Networks: Near-field intrabody communication," *IBM Systems Journal*, 1996.
- [4] M. S. Wegmueller *et al.*, "Signal Transmission by Galvanic Coupling Through the Human Body," *IEEE Trans. Instrum. Meas.*, 2010.
- [5] S. Maity *et al.*, "Bio-Physical Modeling, Characterization, and Optimization of Electro-Quasistatic HBC," *IEEE Trans. Biomed. Eng.*, 2019.
- [6] A. Datta *et al.*, "Channel Modeling for Physically Secure Electro-Quasistatic In-Body to Out-of-Body Communication with Galvanic Tx and Multimodal Rx," in *IEEE Int. Microwave Symposium (IMS)*, 2021.
- [7] M. Riley *et al.*, "Wireless galvanic impulse communication for high-throughput, low-power, miniaturized neuromodulation implants," in *Int. Conf. IEEE Engineering in Medicine & Biology Society (EMBC)*, 2023.
- [8] B. Yuk *et al.*, "An implantable body channel communication system with 3.7-pj/b reception and 34-pj/b transmission efficiencies," *SSC-L*, 2020.
- [9] C. Lee *et al.*, "A miniaturized wireless neural implant with body-coupled power delivery and data transmission," *IEEE J. Solid-State Circ.*, 2022.
- [10] B. Chatterjee *et al.*, "Biphasic quasistatic brain communication for energy-efficient wireless neural implants," *Nat. Electron.*, 2023.
- [11] N. Modak *et al.*, "Bio-Physical Modeling of Galvanic Human Body Communication in EQS Regime," *IEEE Trans. Biomed. Eng.*, 2022.
- [12] S. Gabriel, R. W. Lau, and C. Gabriel, "The dielectric properties of biological tissues: Iii. parametric models for the dielectric spectrum of tissues," *Physics in Medicine and Biology*, 1996.